Receding horizon maneuver generation for automated highway driving

Julia Nilsson,[*♦◇] Paolo Falcone,[◇] Mohammad Ali,[♦] and Jonas Sjöberg[◇]

[♦] *Volvo Car Corporation, Sweden,*
e-mail: {julia.nilsson, mohammad.ali}@volvocars.com
[◇] *Chalmers University of Technology, Sweden,*
e-mail: {paolo.falcone, jonas.sjoberg}@chalmers.se

Abstract

This paper focuses on the problem of decision-making and control in an autonomous driving application for highways. By considering the decision-making and control problem as an obstacle avoidance path planning problem, the paper proposes a novel approach to path planning, which exploits the structured environment of one-way roads. As such, the obstacle avoidance path planning problem is formulated as a convex optimization problem within a receding horizon control framework, as the minimization of the deviation from a desired velocity and lane, subject to a set of constraints introduced to avoid collision with surrounding vehicles, stay within the road boundaries, and abide the physical limitations of the vehicle dynamics. The ability of the proposed approach to generate appropriate traffic dependent maneuvers is demonstrated in simulations considering traffic scenarios on a two-lane, one-way road with one and two surrounding vehicles.

Keywords: Decision-making and control, Obstacle avoidance path planning, Model predictive control, Advanced driver assistance systems, Automated vehicles.

1. Introduction

Besides increasing transport efficiency and driver convenience, automated driving is expected to enhance traffic safety. On highways, a high percentage of traffic accidents and fatalities is caused by human errors in lane change and overtake maneuvers [1]. Advanced Driver Assistance Systems (ADAS) such as Adaptive Cruise Control (ACC) and collision warning with auto brake have been shown to have a positive impact on traffic safety [2]. Thus, the introduction of fully automated systems, capable of safely and autonomously performing lane change and overtake maneuvers on highways, is expected to further contribute to increase traffic safety.

Highways are structured environments with relatively simple and easily maintainable traffic rules. As such, the driving task is quite straightforward, i.e. maintaining a desired velocity while avoiding collision conflicts with surrounding vehicles, and respecting the traffic rules. Hence, in this paper the problem of determining how a vehicle should behave with respect to surrounding vehicles on highways is considered as an obstacle avoidance path planning problem. Several approaches to path planning with obstacle avoidance have been proposed where the most common include, but are not limited to, grid/graph-based methods e.g. A* and D* [3]-[4], randomized sampling-based methods e.g. Rapidly exploring Random Trees (RRTs) [5]-[6], Artificial Potential Fields (APFs) [7], and cost- and utility-based functions [8]-[9].

In grid/graph-based and randomized sampling-based methods, the state space is divided into grid cells or graph nodes which can be assigned obstacle and goal dependent costs, thus allowing the path planning algorithms to find collision free paths by exploring the grid map or graph tree. However, the algorithms can require significant computer resources since the number of grid cells or graph nodes grow exponentially with the dimension of the state space. Moreover, optimality guarantees of these algorithms are only ensured up to the grid/graph resolution.

The general idea of APFs for path planning is to consider the vehicle as a particle moving in a force field where obstacles generate repulsive artificial potentials while goal locations are represented as attractive poten-

[*]Corresponding author.

tials. Despite the method's popularity, APFs do have several drawbacks, including local minima and oscillatory behavior. Many of the successful applications are therefore restricted to environments where objects move at relatively low velocities, where the path planning is performed in order to achieve some well-defined motion task, or where the APF is used as a mean of reacting to unexpected obstacles.

Similar to APFs, cost- and utility-based functions are commonly used due to their straightforwardness and simplicity. By e.g. adding a cost term that increases when obstacles are in close proximity, collision free paths can be determined. However, these types of cost functions and constraints are normally non-linear and/or non-convex, thus providing no guarantee of generating an optimal solution. Further, utility- and cost-based approaches do not normally include a search through the configuration space but rather use the cost functions or constraints as a mean of determining which maneuver to perform within a limited set of predefined paths.

Although the above mentioned approaches for path planning with obstacle avoidance do give good results in a number of applications, they also come with various drawbacks where the main is the trade-off between required computational resources and solution optimality. Further, many of the commonly used obstacle avoidance path planning methods lack formal stability analysis and verification methods and thereby rely heavily on extensive simulation testing. It is therefore desirable to formulate the obstacle avoidance path planning problem as a low complexity problem within a framework where stability analysis and verification tools exists.

In this paper, the obstacle avoidance path planning problem is formulated as a Model Predictive Control (MPC) problem [10]. In the MPC path planning framework, a path is found as the solution of a constrained optimal control problem over a finite time horizon. In particular, a cost function is minimized subject to a set of constraints including the vehicle dynamics, design and physical constraints, and additional constraints introduced to avoid collision with surrounding vehicles. The constrained optimal control problem is solved in receding horizon, i.e. at every time step the problem is formulated over a shifted time horizon, based on new available sensor measurement information. The main advantage of resorting to such a formulation is that collision avoidance is guaranteed, provided that the optimization problem is feasible. However, collision avoidance constraints generally result in mixed-integer inequalities [11], which may lead to prohibitive computational complexity that prevents the real-time execution of the path planning algorithm [12]. A particular optimal control trajectory planning algorithm is therefore general tailored to a certain traffic situation or maneuver [13]-[14].

To accommodate both collision avoidance constraint satisfaction and low computational complexity, in this paper, the collision avoidance constraints are formulated as affine combinations of the vehicle states and inputs. By exploiting the highway structure, two approaches to affinely express the collision avoidance constraints are presented. Thus, the need of mixed-integer inequalities is eliminated and the resulting optimization problem is a standard convex Quadratic Program (QP) that can be solved in real-time by using efficient solvers e.g. [15]. The general idea behind the affine formulation of the collision avoidance constraints was first introduced in [16], and the proposed approach has been shown to produce paths which can be tracked by a four-wheel vehicle model in real-time in [17]. This paper extends the results presented in [16]-[17] by providing further details regarding the affine formulation of the collision avoidance constraints and by applying the MPC path planning algorithm to more complex traffic situations involving two surrounding vehicles.

The remainder of the paper is organized as follows: in Section 2 the standard MPC problem formulation is introduced, while Section 3 presents the problem statement. Section 4 describes the vehicle dynamics model, and the physical and design constraints to which it is subjected. In Section 5 the affine formulation of the collision avoidance constraints is introduced, and the MPC path planning problem is formulated. Simulation results are presented in Section 6, and conclusions are stated in Section 7.

2. Preliminaries

Consider the linear, time-invariant, discrete time system

$$x_{t+1} = Ax_t + Bu_t, \tag{1}$$

where

$$x \in \mathcal{X} \subseteq \mathbb{R}^n,\ u \in \mathcal{U} \subseteq \mathbb{R}^m, \tag{2}$$

are the state and input vectors, respectively, and $\mathcal{X}$ and $\mathcal{U}$ are polytopes containing the origin. Without loss of generality, assume the control objective is to control the state of system (1) to the origin, while fulfilling the state and input constraints (2).

Consider the following cost function

$$J(x_t, \mathcal{U}_t) = \|x_{t+N}\|_P^2 + \sum_{k=0}^{N-1} \|x_{t+k}\|_Q^2 + \|u_{t+k}\|_R^2, \tag{3}$$

where $\mathcal{U}_t \triangleq \left[u_t^T, \ldots, u_{t+N-1}^T\right]^T$, $\|x\|_Q^2 \triangleq x^T Q x$ denotes the weighted, squared 2-norm, $N \in \mathbb{N}^+$ is a finite, discrete time horizon called *the prediction horizon* and $P \in \mathbb{R}^{n\times n}$, $Q \in \mathbb{R}^{n\times n}$, $R \in \mathbb{R}^{m\times m}$ are weighting matrices. In MPC, at every time instant t, the following finite time, constrained optimal control problem is formulated and solved

$$\min_{\mathcal{U}_t} J(x_t, \mathcal{U}_t) \tag{4a}$$

subject to

$$x_{t+k+1} = Ax_{t+k} + Bu_{t+k}, \tag{4b}$$
$$x_{t+k} \in \mathcal{X},\ k = 0, \ldots, N, \tag{4c}$$
$$u_{t+k} \in \mathcal{U},\ k = 0, \ldots, N-1, \tag{4d}$$

and the control input is the state feedback law $u^*(x_t)$ obtained from the first element of the solution $\mathcal{U}_t^*$ to the problem (4). The problem (4) is solved in *receding horizon*, i.e. every time instant the problem (4) is formulated and solved based on the current state x_t, over a shifted time horizon. If the sets $\mathcal{X}$, $\mathcal{U}$ in (4c)-(4d) are convex, then the MPC problem (4) can be equivalently rewritten as a standard QP problem

$$\min_{\mathcal{U}_t} J = \frac{1}{2} w^T H w + d^T w \tag{5a}$$

subject to

$$H_{in} w \leq K_{in}, \tag{5b}$$
$$H_{eq} w = K_{eq}, \tag{5c}$$

with $w \triangleq \left[\mathcal{U}_t, x_t^T, \ldots, x_{t+N}^T\right]^T$. The QP problem (5) is convex if the matrix H is symmetric and positive semi-definite.

3. Problem statement

The problem of autonomous highway driving is considered as the problem of determining how the ego vehicle, E, i.e. the vehicle to be controlled, should behave with respect to the surrounding vehicles, S_j, $\forall j = 1, \ldots, q$ where q is the number of surrounding vehicles. Consider the highway traffic scenario consisting of E, and two surrounding vehicles, S_1 and S_2, as shown in Figure 1. In the scenario, S_1 is driving ahead of E in the same lane, and S_2 is traveling in the left adjacent lane. In the described traffic situation, E could either

1. adjust its velocity in order to follow S_1,
2. accelerate and overtake S_1 in front of S_2 or,
3. wait until S_2 has passed before performing the overtake maneuver.

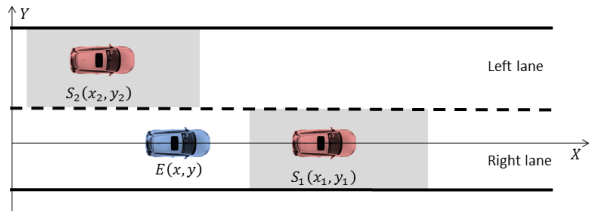

Figure 1: Vehicles traveling on a road with two lanes. The ego vehicle (E) is shown in blue and the surrounding vehicles (S_1 and S_2) in red. The grey boxes around S_1 and S_2 indicate safety critical regions which E should not enter.

The choice of which maneuver to perform is a result of a decision-making process where issues concerning the benefits, efforts, and safety risks associated with the alternative maneuvers must be considered. In order to capture this decision-making process, a path has to be planned for E with the objective of

i) keeping E at its desired velocity $v_{x_{\text{des}}}$ and,

ii) maintaining E at the center-line of its preferred lane y_{ref},

while

a) avoiding collisions with S_1 and S_2,

b) retaining E within the road boundaries, and

c) respecting E's physical and design limitations.

The path planning problem (5) stated in terms of the objectives *(i)-(ii)* and the requirements *(a)-(c)* can be formulated and solved in receding horizon, as follows

$$\min_{\text{path}} \text{cost function} \tag{6a}$$

subject to

$$\text{vehicle dynamics}, \tag{6b}$$
$$\text{physical and design constraints}, \tag{6c}$$
$$\text{collision avoidance constraints}, \tag{6d}$$

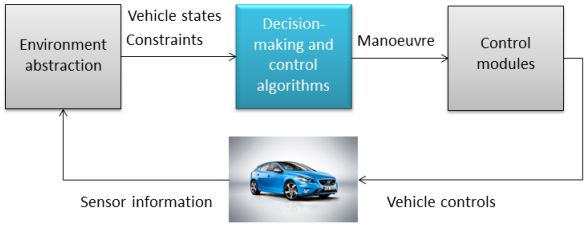

Figure 2: Schematic architecture of the proposed system.

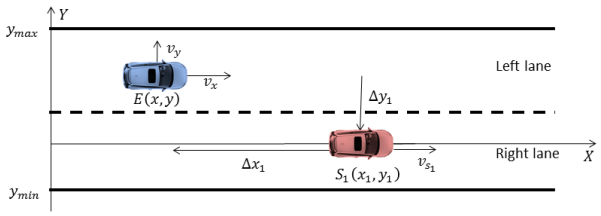

Figure 3: Scenario setup and notation. The ego vehicle (E) is shown in blue while the surrounding vehicle S_1 is displayed in red.

where the cost function (6a) reflects the control objectives *(i)* and *(ii)*, the constraints (6b) and (6c) guarantee that the generated path fulfills the requirements *(b)* and *(c)*, while the constraint (6d) allows for avoiding collisions with S_1 and S_2 according to requirement *(a)*. The path found as the solution of (6), corresponds to the desired maneuver expressed in terms of E's longitudinal and lateral position, velocity, and acceleration denoted by x, y, v_x, v_y, a_x, and a_y respectively.

The problem (6) is formulated based on the following set of assumptions:

A1 E is equipped with low-level control systems capable of tracking the path generated as solution of problem (6).

A2 A sensing system on E is present, which measure its own position within the road and the position and velocity of S_1 and S_2, i.e. all needed measurements are available.

Example of the assumed low-level control system, and the necessary sensing technology are given in [17] and [18], respectively.

A simplified schematic architecture of the proposed system is illustrated in Figure 2. Note that this paper is only concerned with the decision-making and control algorithm (6), in accordance with Assumptions **A1** and **A2**.

4. Modeling

This section presents the simplified point-mass model used in this paper to describe the vehicle dynamics (6b), along with the physical and design constraints (6c).

4.1. Vehicle dynamics

Using the notation introduced in Figure 3, the following set of equations is used to model the motion of E, with respect to S_j, and the road boundaries, in a road aligned coordinate frame,

$$\Delta x_{j_{k+1}} = v_{s_{j_k}} h - v_{x_k} h, \ \forall j = 1, \dots, q, \ k = 0, \dots N, \quad (7a)$$
$$y_{k+1} = y_k + v_{y_k} h, \ \forall k = 0, \dots N, \quad (7b)$$
$$v_{x_{k+1}} = v_{x_k} + a_{x_k} h, \ \forall k = 0, \dots N, \quad (7c)$$
$$v_{y_{k+1}} = v_{y_k} + a_{y_k} h, \ \forall k = 0, \dots N, \quad (7d)$$

where h is the discrete sampling time, v_{s_j} denotes the longitudinal velocity of S_j, and $\Delta x_j = x_{s_j} - x$ denotes the relative distance between S_j and E along the x-axis. The dynamics of the point-mass model can compactly be written as

$$\xi_{k+1} = f(\xi_k, u_k, \tau_k) \quad (8)$$

where $\xi = \left[\Delta x_j, y, v_x, v_y\right]^T$, $u = \left[a_x, a_y\right]^T$ and the disturbance vector $\tau = \left[v_{s_j}\right]^T$. In (8), the control inputs are considered to be the longitudinal and lateral acceleration. However, whether the acceleration, velocity, or position are used as control inputs to the assumed low-level control system i.e. Assumption **A1**, depends on the available vehicle interface.

In equation (7), the lateral and longitudinal positions are independent, i.e. not subject to the vehicle nonholonomic constraints. For instance, $v_x = 0$, $v_y \neq 0$ could generate a lateral movement, that is unfeasible for a vehicle. Nevertheless, equation (7) can generate a path in a Cartesian coordinate system that can be followed by a vehicle, by limiting the side *slip angle*, defined as $\beta = \arctan \frac{v_y}{v_x}$. In particular, by assuming $|\beta| \leq 10°(\approx 0.17\text{rad})$, small angle approximation leads to

$$-0.17 v_{x_k} \leq v_{y_k} \leq 0.17 v_{x_k}, \ \forall k = 0, \dots N. \quad (9)$$

4.2. Physical and design constraints

The system described by (8) is subject to the following set of constraints

$$\xi_{\min} \leq \xi_k \leq \xi_{\max}, \ \forall k = 0, \dots N, \quad (10a)$$
$$u_{\min} \leq u_k \leq u_{\max}, \ \forall k = 0, \dots N, \quad (10b)$$
$$\Delta u_{\min} \leq \Delta u_k \leq \Delta u_{\max}, \ \forall k = 1, \dots N, \quad (10c)$$

where $u_k = \Delta u_k + u_{k-1}$. Inequality (10a) limits the longitudinal velocity so that E remains within the allowed speed limits, and constrains the lateral motion of E to remain within the lane boundaries. Constraint (10b) limits the longitudinal and lateral accelerations, while inequality (10c) bounds the longitudinal and lateral jerks in order to allow for smooth and comfortable maneuvers. Moreover, the inequalities (10b)-(10c) ensure that the planned maneuver is within the capabilities of the low-level control systems in Assumption **A1**.

5. MPC path planning

In this section the path planning problem (6) is formulated in detail. Particularly, the cost function (6a) designed to satisfy objectives *(i)-(ii)*, and two approaches to the formulation of the affine collision avoidance constraints (6d) are presented.

5.1. Cost function

The MPC problem satisfying the objectives *(i)-(ii)* presented in Section 3, can be formulated as the QP in (5) with $w = [\xi_k, u_k, \tau_k]^T$, the vehicle dynamics described by (8), physical and design constraints (9)-(10), and the cost function defined as

$$J = \sum_{k=0}^{N-1} \alpha(v_{x_k} - v_{x_{\text{des}}})^2 + \kappa(y_k - y_{\text{ref}})^2, \tag{11}$$

where α and κ are positive scalar weights. Objectives *(i)-(ii)* are pursued by the terms $\alpha(v_{x_k} - v_{x_{\text{des}}})^2$ and $\kappa(y_k - y_{\text{ref}})^2$ which respectively penalizes deviations from the desired velocity and lane. Further, in order to enforce ride comfort in the design, additional terms such as $\gamma v_{y_k}^2$, $\nu a_{x_k}^2$, and $\varrho a_{y_k}^2$, where γ, ν, and ϱ are positive scalar weights, can be included in (11).

5.2. Collision avoidance constraints

By restricting E to remain outside safety critical regions, as illustrated in Figure 1, it is possible to ensure that E stays on a collision free path. However, as indicated in Figure 1, the area outside the safety critical regions is non-convex. In order to keep the MPC path planning problem within the QP framework (5), the safety constraints should be expressed by affine inequalities. For this reason, each rectangular safety critical region in Figure 1, is approximated by two affine constraints called the Forward Collision Avoidance Constraint (FCC) and the Rear Collision Avoidance Constraint (RCC) shown in Figure 4 and 5 respectively. The purpose of the FCC is to prevent E from colliding with the vehicle ahead in the same lane, while the purpose of the RCC is to avoid collisions with a trailing vehicle when moving to the adjacent lane.

As seen in Figure 4, the FCC can be written as

$$\frac{\Delta x_{j_k}}{L_f} \pm \frac{\Delta y_{j_k}}{W} \geq 1 \;\forall\; k = 0, \ldots, N, \;\; j = 1, \ldots, q, \tag{12}$$

where Δx_j and Δy_j are defined as in Figure 3, with $\Delta y_j = y_{s_j} - y$, and y_{s_j} denotes the lateral position of S_j. The sign of the second term depends on which lane S_j is positioned in (+ if left lane, − if right lane). The parameters L_f and W are set as

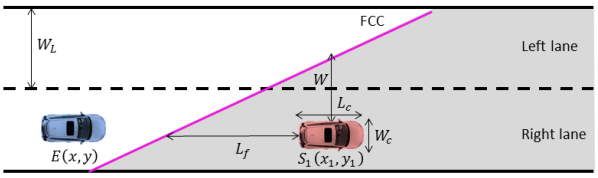

Figure 4: The FCC enforced for a surrounding vehicle, S_1, (red) traveling in the same lane as the ego vehicle, E, (blue). The unfeasible area generated by the FCC is displayed in grey.

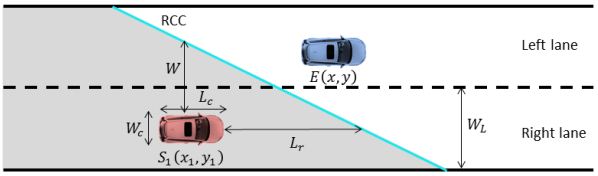

Figure 5: The RCC enforced for a surrounding vehicle, S_1, (red) traveling in the right adjacent lane to the ego vehicle, E, (blue). The unfeasible area generated by the RCC is displayed in grey.

$$L_f = v_{x_k}\theta_f + L_c, \;\forall\; k = 0, \tag{13a}$$

$$W = \frac{1}{2}W_L + W_c, \tag{13b}$$

where θ_f is the desired time gap of E when approaching S_j. The length and width of S_j is respectively denoted by L_c, and W_c, and W_L denotes the lane width. Note that at every instance of (6) L_f is updated according to the current value of v_x. Hence, depending on E's velocity and the minimal safety distance L_c, L_f defines the desired safe distance between E and S_j. Likewise, depending on W_L and W_c, W defines the desired lateral distance which E should maintain to S_j when passing.

Similar to the FCC, the RCC can be written as,

$$\frac{\Delta x_{j_k}}{L_r} \pm \frac{\Delta y_{j_k}}{W} \leq -1 \;\forall\; k = 0, \ldots, N, \;\; j = 1, \ldots, q, \tag{14}$$

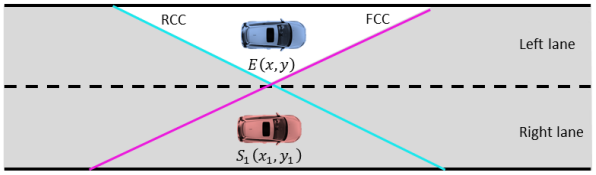

Figure 6: The FCC and RCC simultaneously enforced. The unfeasible area generated by the FCC and RCC is displayed in grey, the ego vehicle, E, is shown in blue while the surrounding vehicle, S_1, is displayed in red.

where the sign of the second term depends on which lane S_j is positioned in (− if left lane, + if right lane), and the parameter L_r is set as

$$L_r = v_{x_k}\theta_r + L_c, \ \forall\ k = 0, \tag{15}$$

where θ_r is the desired time gap of E to the trailing vehicle S_j when moving into the adjacent lane.

However, as illustrated in Figure 6, if both constraints (12) and (14) are simultaneously enforced, E is only allowed to be positioned in a small area adjacent to S_j. Hence, the FCC should only be enforced when E is behind S_j (i.e. for $\Delta x_j > 0$), while the RCC should only be enforced when E is preceding to S_j. In order to avoid simultaneously enforcing the FCC and RCC, the inequalities (12) and (14), are modified by introducing slack variables that relax the FCC and RCC depending on the relative position of E and S_j, i.e. the sign of Δx_j.

The constraints (12) and (14) are therefore rewritten as follows,

$$\frac{\Delta x_{j_k}}{L_f} \pm \frac{\Delta y_{j_k}}{W} + \varepsilon_{x_{j_{f_k}}} \geq 1 \ \forall\ k = 0, \ldots, N,\ j = 1, \ldots, q, \tag{16}$$

where $0 \leq \varepsilon_{x_{j_f}}$ and,

$$\frac{\Delta x_{j_k}}{L_r} \pm \frac{\Delta y_{j_k}}{W} + \varepsilon_{x_{j_{r_k}}} \leq -1 \ \forall\ k = 0, \ldots, N,\ j = 1, \ldots, q, \tag{17}$$

with $\varepsilon_{x_{j_r}} \leq 0$. A non-zero value of $\varepsilon_{x_{j_f}}$ in (16) shifts the line labeled FCC in Figure 4 to the right, thus allowing E to complete the overtake maneuver. Similarly a non-zero value of $\varepsilon_{x_{j_r}}$ in (17) shifts the line labeled RCC in Figure 5 to the left, thus allowing E to either follow S_j or initiate the overtake maneuver.

Note once more that $\varepsilon_{x_{j_f}}$ and $\varepsilon_{x_{j_r}}$ should be non-zero only if $\Delta x_j \leq 0$ and $\Delta x_j \geq 0$, respectively. In the following sections, two approaches are presented and motivated to achieve this objective. The two approaches are based on modifications of the FCC and RCC constraints and the objective function. Benefits and drawbacks of the proposed approaches are discussed and highlighted by the simulation results presented in Section 6.

In the rest of the paper, only two lanes are considered in order to preserve problem convexity. However, without loss of generality, more lanes can be considered by formulating and solving multiple QPs. Further, by only considering two lanes in each QP optimization, the number of surrounding vehicles is consequently limited to approximately 3-4.

5.3. Approach 1 to path planning optimization

In this approach the enforcement of the FCC or RCC is achieved by modifying the cost function (11) and introducing a constraint which defines the relation between the slack variables, $\varepsilon_{x_{j_f}}$, $\varepsilon_{x_{j_r}}$, and the relative distance Δx_j.

The following cost function is considered

$$J_1 = J + \sum_{k=0}^{N-1}\sum_{j=1}^{q} \Upsilon\varepsilon_{x_{j_{f_k}}}^2 + \Phi\varepsilon_{x_{j_{r_k}}}^2, \tag{18}$$

where Υ, and Φ are positive scalar weights, and J is defined as in (11). Further, in addition to the collision avoidance constraints (16)-(17) the following conditions are imposed

$$\Delta x_{j_k} + \varsigma\varepsilon_{x_{j_{f_k}}} \geq 0 \ \forall\ k = 0, \ldots, N,\ j = 1, \ldots, q, \tag{19a}$$

$$\Delta x_{j_k} + \varsigma\varepsilon_{x_{j_{r_k}}} \leq 0 \ \forall\ k = 0, \ldots, N,\ j = 1, \ldots, q, \tag{19b}$$

where ς is a positive constant. The cost terms in (18) favor $\varepsilon_{x_{j_f}}$ and $\varepsilon_{x_{j_r}}$ to be zero unless required by conditions (19).

The resulting QP path planning optimization problem can thus be formulated as

$$\min_{\mathcal{U}_k} J_1 \tag{20a}$$

subject to

$$(8), (9), (10), (16), (17), (19), \tag{20b}$$

where $\mathcal{U}_k = \left[u_k^T, \ldots, u_{k+N-1}^T\right]^T$ and $u_k = \left[a_{x_k}, a_{y_k}, \varepsilon_{x_{j_{f_k}}}, \varepsilon_{x_{j_{r_k}}}\right]$.

Alternatively, consider a cost function formulated as

$$\begin{aligned} J_{ex_1} = J + \sum_{k=0}^{N-1}\sum_{j=1}^{q} &\Upsilon\varepsilon_{x_{j_{f_k}}}^2 + \Phi\varepsilon_{x_{j_{r_k}}}^2 + \\ &\Psi\Delta x_{j_k}\varepsilon_{x_{j_{f_k}}} + \Omega\Delta x_{j_k}\varepsilon_{x_{j_{r_k}}}, \end{aligned} \tag{21}$$

where J is defined as in (11) and Υ, Φ, Ψ, and Ω are positive scalar weights. If the cost J_{ex_1} is minimized, the terms $\Delta x_j\varepsilon_{x_{j_f}}$ and $\Delta x_j\varepsilon_{x_{j_r}}$ force $\varepsilon_{x_{j_f}}$ and $\varepsilon_{x_{j_r}}$ to be non-zero as $\Delta x_j \leq 0$ and $\Delta x_j \geq 0$ respectively, thus rendering (19) superfluous. However, although the minimization of (21) subject to (7), (9), (10), (16)-(17), can be written as in (5) with $w = \left[\xi_k, u_k, \tau_k, \varepsilon_{x_{j_{f_k}}}, \varepsilon_{x_{j_{r_k}}}\right]^T$, where $\tau = \left[v_{s_j}, y_{s_j}\right]^T$ the problem is not convex since the resulting H in (5) is not positive semi-definite and the cost (21) is unbounded below. Positive semi-definiteness of H can be achieved by adding the term Δx_j^2 in the cost function (21) as following

$$\begin{aligned} J_{ex_2} = J + \sum_{k=0}^{N-1}\sum_{j=1}^{q} &\Upsilon\varepsilon_{x_{j_{f_k}}}^2 + \Phi\varepsilon_{x_{j_{r_k}}}^2 + \Psi\Delta x_{j_k}\varepsilon_{x_{j_{f_k}}} + \\ &\Omega\Delta x_{j_k}\varepsilon_{x_{j_{r_k}}} + \Lambda\Delta x_{j_k}^2, \end{aligned} \tag{22}$$

where Λ is positive scalar. However, introducing the Δx_j^2 term in the cost function (22), incentives E to stay close to S_j since the relative distance is penalized. This conflicts with the objective of maintaining safety margins to S_j in order to avoid collisions. Also, minimization of the relative distance Δx_j can cause an undesirable behavior where E adapts to the velocity of S_j rather than maintaining its desired velocity. For this reason it is preferable to enforce the FCC and RCC constraints by the cost function (18) and the constraints (16)-(17), (19) rather than solely by the cost function (22).

Remark 1. *The effectiveness of this approach is strongly affected by the parameter tuning since although the slack variables assume non-zero values depending on the value of Δx_j there is no guarantee that the slack variables will not assume a non-zero value when undesirable, i.e. $\varepsilon_{x_{j_f}}$ and $\varepsilon_{x_{j_r}}$ can be non-zero although $\Delta x_j \geq 0$ and $\Delta x_j \leq 0$, respectively.*

Remark 2. *The optimization problem* (20)*, consists of* $(2 + 2q)N$ *optimization variables i.e. control inputs and slack variables, and* $(19 + 7q)N$ *constraints corresponding to system dynamics* (8)-(9)*, physical and design constraints* (10)*, as well as collision avoidance constraints* (16)-(17)*, and* (19)*.*

5.4. Approach 2 to path planning optimization

In order to guarantee collision avoidance, if in fact a collision free path exists, the collision avoidance constraints must be appropriately enforced as described in Section 5.2. As mentioned in Remark 1, a problem when introducing slack variables is to properly weight them in the cost function, which for general scenarios can be difficult to achieve. For that reason, in this approach the problem of deciding when the FCC and RCC should be enforced is removed from the cost function and instead incorporated into the problem solely through a set of constraints. As such, the FCC is only allowed to be relaxed if E has either changed lanes or passed S_j. To achieve this, the FCC (16) is redefined as

$$\begin{aligned} \frac{\Delta x_{j_k}}{L_f} \pm \frac{\Delta y_{j_k}}{W} + \vartheta_j \varepsilon_{x_{j_f}} + \frac{\varepsilon_{y_{j_k}}}{\varphi_j} + \varepsilon_{j_{f_k}} \geq 1, \\ \forall\ k = 0, \ldots, N,\ j = 1, \ldots, q, \end{aligned} \tag{23}$$

where the purpose of the $\vartheta_j \varepsilon_{x_{j_f}}$ term is to relax the FCC if E has passed S_j, the purpose of the $\frac{\varepsilon_{y_{j_k}}}{\varphi_j}$ term is to relax the FCC if E has changed lanes, and the term ε_{j_f} should only relax the FCC if no other feasible options exist.

Since $\varepsilon_{x_{j_f}} \geq 0$, by letting ϑ_j be initialized prior to each instance of (6) as

$$\vartheta_j = -sgn(\Delta x_{j_k}),\ \forall\ k = 0,\ j = 1, \ldots, q, \tag{24}$$

the $\vartheta_j \varepsilon_{x_{j_f}}$ term will only relax (23) if E has physically passed S_j rendering $\Delta x_j < 0$.

If $\sigma_{l,r}$ denotes the lane center adjacent to S_j's lane, i.e. σ_l is left adjacent and σ_r is right adjacent, by setting

$$\varepsilon_{y_{j_k}} = -\Delta y_{j_k} - \sigma_{l,r},\ \forall\ k = 0, \ldots, N,\ j = 1, \ldots, q, \tag{25}$$

$\varepsilon_{y_j} \geq 0$ if and only if $y \geq \sigma_{l,r} \Leftrightarrow \Delta y_j \leq -\sigma_{l,r}$. The variable ε_{y_j} will thus only relax the FCC if E has changed lanes. The parameter φ_j is initialized prior to each instance of (6) as

$$\varphi_j = \max(\psi, |\Delta x_{j_k}|),\ \forall\ k = 0,\ j = 1, \ldots, q, \tag{26}$$

in order to reduce the impact of $\varepsilon_{y_j} < 0$. The parameter $\psi \geq 0$ is included in order to avoid division with small or zero values.

The slack variable $\varepsilon_{j_f} \geq 0$ should be heavily penalized in the cost function in order to only affect condition (23) if no other feasible options exist. An example of such a scenario if the optimization problem (6) is initialized in the unfeasible region i.e. the grey area in Figures 4-5 due to. e.g. sensor measurement errors.

Hence, over the prediction horizon the FCC (23) is only relaxed by ε_{y_j} (and ε_{j_f}), while $\varepsilon_{x_{j_f}}$ functions as a decision variable that determines whether the constraint should be active depending on the physical position of E.

The RCC (17) can likewise be reformulated as

$$\begin{aligned} \frac{\Delta x_{j_k}}{L_r} \pm \frac{\Delta y_{j_k}}{W} - \vartheta_j \varepsilon_{x_{j_r}} - \varepsilon_{y_{j_k}} + \varepsilon_{j_{r_k}} \leq -1, \\ \forall\ k = 0, \ldots, N,\ j = 1, \ldots, q, \end{aligned} \tag{27}$$

where $\varepsilon_{j_r} \leq 0$. The cost function is set as

$$J_2 = J + \sum_{k=0}^{N-1} \sum_{j=1}^{q} \chi \varepsilon_{j_{f_k}}^2 + \Xi \varepsilon_{j_{r_k}}^2, \tag{28}$$

where χ and Ξ are positive scalar weights. The resulting path planning optimization problem for this approach can thus be formulated as follows

$$\min_{\mathcal{U}_k} J_2 \tag{29a}$$

subject to

$$(8), (9), (10), (23), (27), \tag{29b}$$

where $\mathcal{U}_k = \left[u_k^T, \ldots, u_{k+N-1}^T\right]^T$ and $u_k = \left[a_{x_k}, a_{y_k}, \varepsilon_{x_{j_f}}, \varepsilon_{y_{j_k}}, \varepsilon_{x_{j_r}}, \varepsilon_{j_{f_k}}, \varepsilon_{j_{r_k}}\right]$.

Remark 3. *The main advantage of this approach is that since the FCC and RCC are only relaxed over the prediction horizon when* E *is in the adjacent lane, the optimization problem* (29) *is less sensitive to parameter tuning in order to generate appropriate collision free maneuvers. This is a main advantage compared to Approach 1 since in that approach, a correct parameter tuning is essential for the algorithm's performance as mentioned in Remark 1.*

On the other hand, the main drawback of formulating the collision avoidance constraints according to (23) *and* (27)*, is that during an optimization cycle a full overtake maneuver can never be planned. This is because over the prediction horizon, the FCC is only relaxed when* E *is in the adjacent lane. Hence, only when* E *has physically passed* S_j*, rendering* $\Delta x_j < 0$ *i.e.* $\varepsilon_{x_{j_f}} > 0$ *is it allowed to return to its original lane. The same logic applies to the formulation of the RCC.*

Remark 4. *The optimization problem* (29)*, consists of* $(2 + 3q)N + 2q$ *optimization variables i.e. control inputs, and slack variables, and* $(19 + 4q)N + 2q$ *constraints corresponding to system dynamics* (8)-(9)*, physical and design constraints* (10)*, as well as collision avoidance constraints* (23)*,* (25)*, and* (27)*.*

6. Simulation results

This section presents and explains simulation results for the MPC obstacle avoidance path planning algorithms highlighting the main benefits and drawbacks of the path planning problem formulations presented in Section 5. Section 6.1 presents simulation results of the path planning algorithms of Approach 1 and Approach 2 applied to a simple traffic situation with one surrounding vehicle. Some important aspects and tuning issues of Approach 2 for path planning are discussed in Section 6.2. In Section 6.3 simulation results of the path planning algorithm of Approach 2 applied on traffic scenarios on a two-lane, one-way road with two surrounding vehicles are presented. In Section 6.1 and 6.3, the proposed approaches for obstacle avoidance path planning are applied to a point-mass simulation model, and implemented by solving in receding horizon the optimization problems (20), and (29) using the Matlab optimization routine `quadprog`. Section 6.4 extends on the simulation results presented in Section 6.1 by applying the MPC obstacle avoidance path planning algorithm of Approach 2 to a four wheel vehicle simulation model.

Table 1: Initial conditions for the two considered scenarios with one surrounding vehicle.

	Scenario 1	Scenario 2
Δx_1 [m]	50	50
y [m]	0	0
v_x [m/s]	20	20
v_y [m/s]	0	0
a_x [m/s^2]	0	0
a_y [m/s^2]	0	0
v_{s_1} [m/s]	15	10
y_{s_1} [m]	0	0

Table 2: General design parameters for the path planning algorithm.

$y_{\max} = 7.5$	$y_{\min} = -2.5$
$v_{y_{\max}} = 5$ m/s	$v_{y_{\min}} = -5$ m/s
$v_{x_{\max}} = 25$ m/s	$v_{x_{\min}} = 0$ m/s
$a_{x_{\max}} = 2$ m/s^2	$a_{x_{\min}} = -4$ m/s^2
$a_{y_{\max}} = 2$ m/s^2	$a_{y_{\min}} = -2$ m/s^2
$\Delta a_{x_{\max}} = 1.5$ m/s^2	$\Delta a_{x_{\min}} = -3$ m/s^2
$\Delta a_{y_{\max}} = 0.5$ m/s^2	$\Delta a_{y_{\min}} = -0.5$ m/s^2
$\theta_f = 2$ s	$\theta_r = 1$ s
$L_c = 5$ m	$W_c = 2.5$ m
$\sigma_l = 5$	$\sigma_r = 0$
$W_L = 5$ m	$\varsigma = 2L_f$
$N = 50$	$h = 0.1$ s

6.1. One surrounding vehicle

A simple traffic situation is considered, where E is driving on a straight two-lane, one-way road with one preceding vehicle S_1. Two scenarios, hereafter referred to as *Scenario 1* and *2* are considered, where E is approaching S_1 with a relative velocity that in Scenario 2 is much larger than in Scenario 1.

For all scenarios it is assumed that E initially travels in its preferred lane, i.e. the right lane corresponding to $y_{\text{ref}} = 0$, at its desired velocity, $v_{x_{\text{des}}} = 20$ m/s. Further, it is assumed that S_1 is traveling in the right lane at constant velocity over the prediction horizon. This is a simplicity assumption purely in order to easily illustrate the path planning algorithms.

For each of the described scenarios the respective initial conditions are given in Table 1. The general design parameters for the decision and control algorithms are given in Table 2 and the design parameters for each approach are given in Table 3.

Table 3: Design parameters for the path planning algorithm using Approach 1-2.

	App. 1	App. 2
α	1	10
κ	0.5	2
γ	1	2
ν	0.5	0.5
ϱ	0.5	0.5
Υ	Δx_{1_0}	NA
Φ	Δx_{1_0}	NA
χ	NA	10000
Ξ	NA	10000

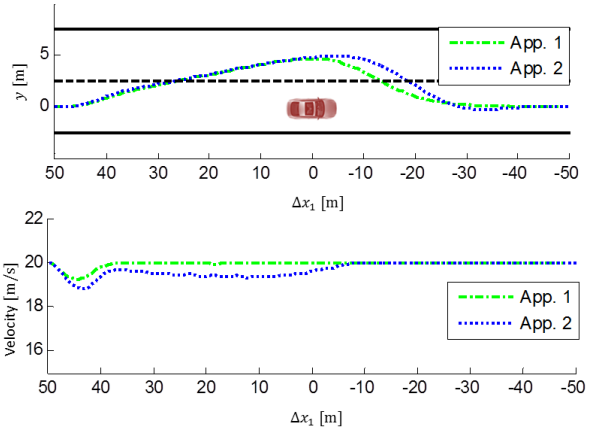

Figure 7: The position trajectory of E relative to S_1, as well as the velocity profile of E for Scenario 1.

In Figures 7-8 the position trajectory of E relative to S_1, as well as the velocity profile of E are shown for the two approaches applied to the two scenarios. The upper plot of each figure can be considered as snapshots of E during the entire maneuver since each dot on the position trajectory of E show the position of E relative to S_1 at the corresponding time instance. From the Figures 7-8 it can be seen that for Scenario 1 and 2, both Approach 1 and 2 generate an appropriate behavior for E, i.e. in order to maintain its desired velocity, E performs an overtake maneuver of S_1 while keeping a safe distance as defined in (13) and (15) throughout the maneuver.

Since a main motivation for ADAS for highway driving is its potential to increase traffic safety, it is crucial that the path planning algorithms ensure safe maneuvers. Although Approach 1 has been shown to provide promising results, for the sake of clarity only Approach 2 will be considered in the following. This is because of, as mentioned in Remark 3, the formulation of

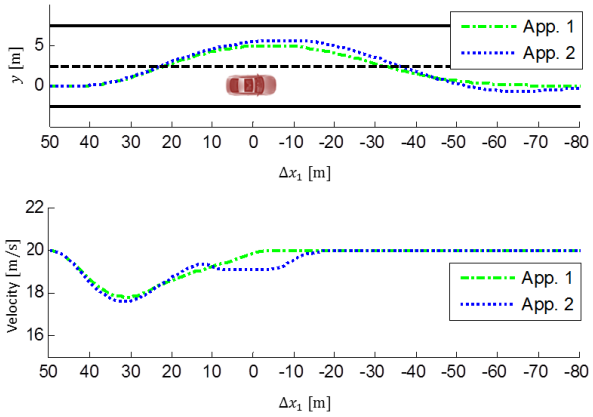

Figure 8: The position trajectory of E relative to S_1, as well as the velocity profile of E for Scenario 2.

the FCC (23) and RCC (27) in Approach 2 renders the approach less sensitive to parameter tuning compared to Approach 1. Hence, Approach 2 is the only approach which generates collision free maneuvers without relying heavily on parameter tuning. However in contrast to Approach 1, a drawback of Approach 2 is that a full overtake maneuver can not be considered during an optimization cycle. Hence, Approach 2 is considered under the assumption that an overtake maneuver can be planned as two separate lane change maneuvers i.e. when initializing the overtake maneuver there is no guarantee that E can return to its original lane.

6.2. *Tuning of the path planning algorithm*

In Table 2 the bounds on y are set to correspond with road boundaries, and the parameters σ_l, σ_r and W_L are set accordingly. The bounds on $v_y, a_x, a_y, \Delta a_x, \Delta a_y$ are set to correspond with the assumed low level control systems i.e. Assumption **A1**, the bounds on v_x are set to correspond with realistic sensor requirements i.e. Assumption **A2**. L_c and W_c are set based on a standard vehicle, and the desired time gaps θ_f and θ_r are set based on desired safety distance related to e.g. vehicle capability and driver preference. The prediction horizon N and the discrete sampling time h provides a prediction time of 5 s, which is deemed reasonable given the simplified assumption regarding the behavior of the surrounding vehicle i.e. constant velocity without performing lane changes.

As shown in Figures 7-8, the velocity of E is reduced right before initializing the overtake maneuver. This is an appropriate behavior when it comes to limiting the relative velocity of the slower moving vehicle S_1 and E,

when E passes S_1. However, although the relative velocity in an overtaking maneuver should generally be limited to ensure safe overtaking, it can be seen that E overly reduces its velocity when performing the overtake maneuver. Analysis of the open loop predictions has shown that this behavior is foremost a consequence of the FCC (23) not being sufficiently relaxed over the prediction horizon.

As mentioned in Remark 3, the FCC is only relaxed by the ε_{y_j} term over the prediction horizon, i.e. once E is in the adjacent lane to S_j. In order to compensate for the insufficient relaxation of the FCC without compromising the safety margins, two approaches to tuning the parameters of (29) can be done.

In particular, the weight χ in (28) can be varied over the prediction horizon such that the cost of using ε_{j_f} to relax the FCC decreases over the prediction horizon. Alternatively, the parameter W can be initialized before each instance of the problem (29) depending on the current lateral position of E, thus varying the slope of the FCC. However, both these approaches should be handled carefully in order to not compromise the safety margins posed by the FCC.

An important aspect of the RCC (27) is apparent when considering a traffic situation where S_j is approaching E at a velocity above the velocity of E, with the intention of passing E. Since the purpose of the RCC is to avoid collisions between E and trailing vehicles S_j, E must be in front of the RCC i.e. ahead of S_j over the prediction horizon. Hence, for S_j to be able to pass E over the prediction horizon, the RCC must be relaxed. As described in Remark 3 in terms of the FCC, the RCC is similarly only relaxed by the ε_{y_j} term over the prediction horizon, which is insufficient when the relative velocity is large. The only other option for relaxing the RCC is by the ε_{j_r} variable, but the high cost associated with relaxing the RCC in this manner can cause a behavior where E adjusts its velocity to S_j rather than allowing it to pass. This results in an inappropriate and dangerous behavior where E always wants to stay ahead of S_j irrespective of the traffic situation. In order to diminish this undesirable behavior, two approaches for compensating for the insufficient relaxation of the RCC without compromising the safety margins are suggested.

Similarly as for the FCC the weight Ξ in (28) can be varied over the prediction horizon such that the cost of using ε_{j_r} to relax the RCC increases over the prediction horizon. Secondly, the scaling parameter L_r can be determined based on the current lateral position of E. Hence, the RCC can be elongated over the x-axis depending on Δy_j which reduces the need to relax the constraint while the safety margins still remains.

Table 4: Initial conditions for the three considered scenarios with two surrounding vehicles.

	Scenario I	Scenario II	Scenario III
Δx_1 [m]	50	50	50
Δx_2 [m]	-20	-20	-20
y [m]	0	0	0
v_x [m/s]	20	20	20
v_y [m/s]	0	0	0
a_x [m/s^2]	0	0	0
a_y [m/s^2]	0	0	0
v_{s_1} [m/s]	15	15	15
y_{s_1} [m]	0	0	0
v_{s_2} [m/s]	17	22	27
y_{s_2} [m]	5	5	5

Table 5: Design and weight parameters of Approach 2, applied to the scenario with two surrounding vehicles.

$\alpha = 10$	$\chi = 1000, k = \{0, \dots, N/2\}$
$\kappa = 2$	$\chi = 100, k = \{N/2+1, \dots, N\}$
$\gamma = 2$	$\Xi = 100, k = \{0, \dots, N/2\}$
$\nu = 0.5$	$\Xi = 1000, k = \{N/2+1, \dots, N\}$
$\varrho = 0.5$	$L_r = L_c + \max(v_x, v_x\lvert\sigma_l - y\rvert)\theta_r$

6.3. Two surrounding vehicles

In order to further study Approach 2, a slightly more complex traffic situation than the scenarios in Section 6.1 is considered. In this section, Scenario 1 in Section 6.1 is extended by introducing a second surrounding vehicle, S_2, traveling in the left lane while as in Scenario 1, E is approaching S_1 which is traveling in the right lane at a velocity below E's desired velocity. In order to examine how S_2 affects the behavior of E three versions of this traffic situation are considered:

I) S_2 is approaching E with a velocity below E's desired velocity.

II) S_2 is approaching E with a velocity similar to E's desired velocity.

III) S_2 is approaching E with a velocity much higher than E's desired velocity.

As in Section 6.1, forsake of clarity it assumed in all scenarios that the vehicles are driving on a straight two-lane, one-way road, and that E initially travels at its desired velocity, ($v_{x_{\text{des}}} = 20$ m/s), in the right lane,

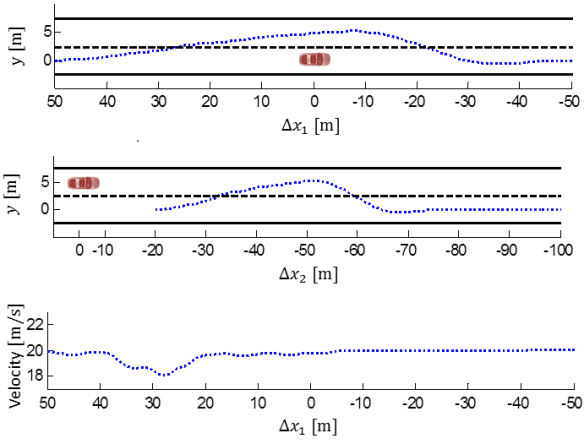

Figure 9: The position trajectory of E relative to S_1 and S_2, as well as the velocity profile of E for Scenario I.

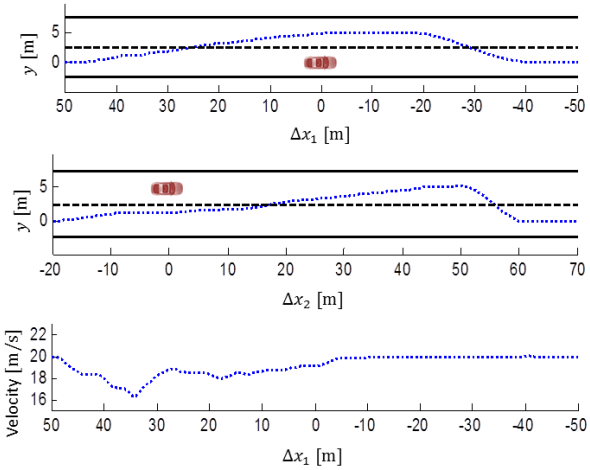

Figure 10: The position trajectory of E relative to S_1 and S_2, as well as the velocity profile of E for Scenario II.

($y_{\text{ref}} = 0$). Further, over the prediction horizon it is assumed that S_j ($j = \{1, 2\}$) are traveling at constant velocity without performing any lane change maneuvers.

For each of the scenarios the respective initial conditions are given in Table 4. The general design parameters for the path planning algorithm are provided in Table 2 and the design and weight parameters of Approach 2 are given in Table 5. As shown in Table 5, in order to sufficiently relax the FCC (as mentioned in Section 6.2) the weight χ is reduced over the prediction horizon. Likewise, regarding the RCC, Table 5 shows that the weight Ξ is increased over the prediction horizon and L_r is initialized depending on the lateral position of E.

As shown in Figures 9-11, E appropriately adjusts its behavior depending on the surrounding traffic situation. In the top figures of Figures 9-11 it can be seen that E overtakes S_1 while maintaining a safe distance as defined in (13) and (15). In the middle figure of Figure 9 it can be seen that E is positioned ahead of S_2 i.e. $\Delta x_2 < 0$ throughout the scenario, while in the middle figures of Figures 10-11 it can be seen that E allows S_2 to pass i.e. $\Delta x_2 > 0$ before moving into the left lane. In both Scenario II and III, E reduces its velocity in order to allow S_2 to pass before overtaking S_1. The velocity of E is most reduced in Scenario II since E must adjust its velocity to S_1 while allowing S_2 to pass. Since the velocity of S_2 is less in Scenario II than in Scenario III the passing maneuver takes longer time, thus forcing E to reduce its velocity during a longer time than in Scenario III.

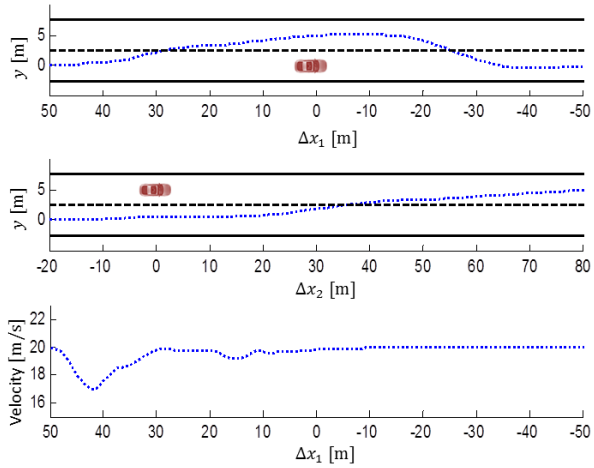

Figure 11: The position trajectory of E relative to S_1 and S_2, as well as the velocity profile of E for Scenario III.

6.4. Path planning and vehicle control

In order to investigate the ability of the proposed approach to obstacle avoidance path planning to compute appropriate, traffic-dependent paths which can be tracked by a low-level controller, a two-level architecture for path planning and vehicle control has been implemented as illustrated in Fig. 12. The high-level path planner (29) computes the desired path while the low-level controller utilizes a non-linear four wheel vehicle model in order to compute the vehicle control inputs required to execute the planned path. Both the high-level planner and low-level controller are formulated as MPC problems where at each time instance an optimal input sequence is calculated by solving a constrained finite time optimal control problem. The optimization prob-

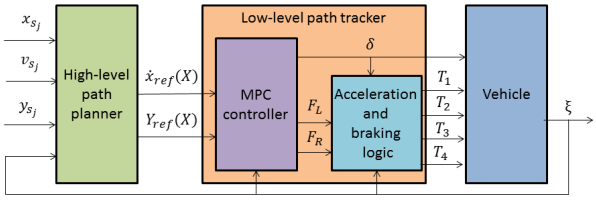

Figure 12: Two-level hierarchical architecture for path planning and vehicle control.

lem is solved in receding horizon i.e. the computed input sequence is only applied during the following sampling interval after which the problem is reformulated and resolved based on the current state and sensor measurements.

The closed loop system is simulated using Matlab Simulink where the high-level path planning and low-level control MPC optimization problems have been implemented as C-coded s-Functions. For the high-level planner (29) CVXGEN [15] is used. The commercial NPSOL software package [19] is used for solving the non-linear low-level control problem. The first element of the optimized control sequence is passed to an external block which uses a four wheel vehicle model and Pacjeka tire model to simulate the vehicle dynamics, and feeds the current state of the vehicle back to the high- and low-level optimization blocks, as shown in Fig. 12.

Considering the two same scenarios as described in Section 6.1, Figures 13-14 respectively shows the position trajectory of E relative to S_1, as well as the velocity profile of E for the two scenarios. In each figure both the planned path using the simple point-mass vehicle model and the resulting path of the four wheel vehicle model are shown, and it can be seen that low-level vehicle controller is able to track the planned paths with only a slight mismatch.

When comparing the planned paths in Figures 7-8 to the paths in Figures 13-14, there is difference although the considered scenarios are the same. This difference is a result of different parameter values resulting from variations in the open and closed loop simulation implementations. Further details concerning the hierarchical, two-level architecture for path planning and vehicle control and corresponding closed loop implementation are given in [17].

7. Conclusions

This paper presents a high-level control scheme for low complexity predictive maneuver generation for automated highway driving. The problem of determining a collision free maneuver in terms of a sequence of longitudinal and lateral control inputs, is formulated as an obstacle avoidance path planning problem in the Model Predictive Control framework. By exploiting the structured environment of one-way roads, collision avoidance constraints are expressed affinely, thus allowing the path planning problem to be formulated as a convex Quadratic Program.

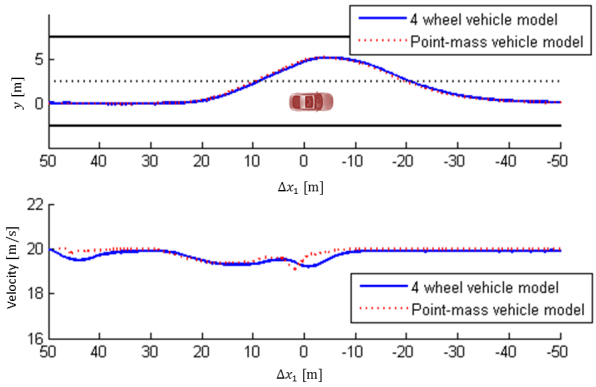

Figure 13: The position trajectory of E relative to S_1, as well as the velocity profile of E for Scenario 1.

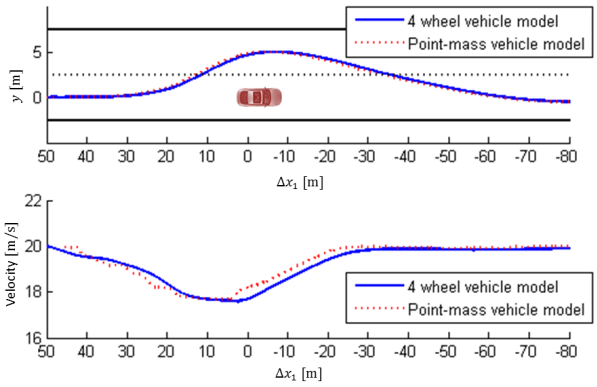

Figure 14: The position trajectory of E relative to S_1, as well as the velocity profile of E for Scenario 2.

Simulation results demonstrate the ability of the presented approach for path planning with affinely formulated collision avoidance constraints to generate traffic dependent collision free maneuvers, which that can be tracked by a low-level vehicle controller.

These results motivate further work to incorporate a dynamic prediction model of the surrounding vehicles, and also include sensor noise and uncertainty. Further, efforts should be made towards a real-time vehicle implementation to evaluate the proposed algorithms in real

world scenarios.

References

[1] M. van Schijndel et al. “Definition of Necessary Vehicle and Infrastructure Systems for Automated Driving”, European commission, June, 2011.

[2] V. L. Neale et al. “An Overview of the 100 Car Naturalistic Study and Findings”, *Proceedings of the 19th International Technical Conference on the Enhanced Safety of Vehicles*, paper 05-0400, 2005.

[3] D. Ferguson, M. Likhachev, and A. Stentz, “A Guide to Heuristic-based Path Planning”, *Proceedings of the Workshop on Planning under Uncertainty for Autonomous Systems at The International Conference on Automated Planning and Scheduling (ICAPS)*, 2005.

[4] J. Ziegler, M. Werling, and J. Schröder, “Navigating Car-like Robots in Unstructured Environments Using an Obstacle Sensitive Cost Function”, *IEEE Intelligent Vehicle Symposium*, pp. 787-791, June, 2008.

[5] S. Karaman, and E. Frazzoli, “Sampling-based Algorithms for Optimal Motion Planning”, *The International Journal of Robotics Research*, vol. 30, no. 7, pp. 846-894, 2011.

[6] Y. Kuwata et al. “Motion Planning for Urban Driving Using RRT”, *IEEE/RSJ International Conference on Intelligent Robots and Systems*, pp. 1681-1686, September, 2008.

[7] O. Khatib, “Real-time Obstacle Avoidance for Manipulators and Mobile Robots”, *The International Journal of Robotics Research*, vol. 5, no. 1, pp. 90-98, 1986.

[8] J. Wei, J. M. Dolan, and B. Litkouhi, “A Prediction- and Cost Function-based Algorithm for Robust Autonomous Freeway Driving”, *IEEE Intelligent Vehicles Symposium*, pp. 512-517, June, 2010.

[9] F. Wang, M. Yang, and R. Yang, “Conflict-Probability-Estimation-Based Overtaking”, *IEEE Transactions on Intelligent Transport Systems*, vol. 10, no. 2, pp. 366-370, June, 2009.

[10] D. Q. Mayne et al. “Constrained Model Predictive Control : Stability and Optimality”, *Automatica*, vol. 36, pp. 789-814, 2000.

[11] F. Borrelli et al. “MILP and NLP Techniques for Centralized Trajectory Planning of Multiple Unmanned Air Vehicles,” *American Control Conference*, pp. 5764-5769, 2006.

[12] S. Wei, M. Zefran, and R. A. DeCarlo, “Optimal Control of Robotic Systems with Logical Constraints: Application to UAV Path Planning”, *IEEE International Conference on Robotics and Automation*, pp. 176-181, May, 2008.

[13] R. Attia et al. “Reference Generation and Control Strategy for Automated Vehicle Guidance”, *IEEE Intelligent Vehicles Symposium*, pp. 389-394, 2012.

[14] J. Daniel et al. “Navigation-based Constrained Trajectory Generation for Advanced Driver Assistance Systems”, *International Journal of Vehicle Autonomous Systems*, vol. 9, no. 3, pp. 269-296, 2011.

[15] J. Mattingley and S. Boyd, “CVXGEN: A Code Generator for Embedded Convex Optimization”, *Optimization and Engineering*, vol. 13, no. 1, pp. 1-27, 2012.

[16] J. Nilsson et al. “Predictive Manoeuvre Generation for Automated Driving”, *IEEE Conference on Intelligent Transportation Systems*, pp. 418-423, October, 2013.

[17] J. Nilsson et al. “Manoeuvre Generation and Control for Automated Highway Driving”, *The 19th World Congress of the International Federation of Automatic Control (IFAC), August, 2014.*

[18] J. Jansson, “Collision Avoidance Theory with Application to Automotive Collision Mitigation”, Ph.D. Thesis, Linköping University, 2005.

[19] P. Gill et al. *NPSOL-Nonlinear Programming Software*, Stanford Business Software, Inc., Mountain View, CA.